

Influence of Stress Ratio on Fatigue Crack Propagation Behavior of Stainless Steel Welds

Crack initiation and growth rates in relation to residual stresses were studied in gas metal arc welds of 316L

BY C. S. KUSKO, J. N. DUPONT, AND A. R. MARDER

ABSTRACT. The fatigue crack propagation behavior of 316L stainless steel gas metal arc welds has been investigated using the K-increasing testing procedure. A series of stress ratios from 0.10 to 0.80 was investigated in order to observe the influence of stress ratio and stress intensity range on the fatigue crack growth rate. A stress ratio of 0.55 has been shown to overcome closure for all the gas metal arc welds tested. Crack closure measurements obtained through the compliance offset method were utilized to explain the increase in crack growth rate and decrease of crack closure as the stress ratio is increased. The increase in fatigue crack growth rate, which occurs as the stress ratio is increased from 0.10 to 0.55, is generally attributed to an extrinsic crack opening effect in which higher stress ratios promote a fully open crack and corresponding higher growth rates. Continued increase in the crack growth rate that occurs as the stress ratio is increased further from 0.55 to 0.70 is attributed to a true intrinsic material response to increasing stress ratio.

Introduction

Conventional arc welds can represent stress concentrations in load-bearing structures because of geometry changes and defects associated with welding. Since welding serves as a prominent joining process for many structural applications, weld-related features can aid in the initiation of cracks. When considered in conjunction with welding residual stresses, propagation of such cracks can become a concern during service. Consequently, an understanding of the fatigue crack propagation behavior of welds is important. Maddox (Ref. 1) and Parry et al. (Ref. 2) have shown that the fatigue crack growth

behavior of welds can be characterized by the well-known Paris equation, which relates the fatigue crack growth rate, da/dN , to the stress intensity range, ΔK (Ref. 3)

$$\frac{da}{dN} = C(\Delta K)^n \quad (1)$$

where a is the crack length, N is the number of cycles, and C and n are material constants. The stress intensity range, ΔK , is given by the difference between the maximum and minimum applied stress intensity of the load cycle, $\Delta K = K_{\max} - K_{\min}$. While the stress intensity range is the main factor that governs the crack growth rate, the stress ratio, R , (ratio of minimum to maximum applied stress intensity) can also influence the crack growth rate. The resulting effect of an increase of R on da/dN has been investigated for wrought stainless steels (Ref. 4), carbon steels (Ref. 5), alloy steels (Refs. 6–8), aluminum (Refs. 9–12), and titanium alloys (Ref. 9). Generally, an increase in R results in an increase in da/dN for a given stress intensity range, ΔK . This influence of R can essentially come from two sources — a true material dependence of crack growth rate on R (i.e., an intrinsic material effect) and/or a crack closure effect. Crack closure refers to the condition in which the crack is not fully open during the entire loading cycle. In this condition, only a portion of the applied stress serves to drive crack propagation. Crack closure is most often attributed to residual stresses. For example, if the crack enters into a compressive stress field, the compressive stress will counteract the applied tensile stress. If the compressive stress is

larger than the minimum applied stress, then the crack may remain closed during a portion of the load cycle. In this case, it is useful to identify an opening stress intensity value, K_{op} , where K_{op} represents the minimum stress intensity required to keep the crack fully open. In short, if the minimum applied stress intensity, K_{\min} , is below K_{op} , then the crack will be closed whenever the applied stress intensity drops below K_{op} . Under this condition, the fully applied stress intensity range, ΔK , does not contribute to crack propagation, and it is useful to define an effective stress intensity range, ΔK_{eff} , where ΔK_{eff} is given by $K_{\max} - K_{\text{op}}$. Under this condition, ΔK_{eff} represents the true driving force for crack propagation. Lastly, it is important to note that one cannot separate an intrinsic crack growth rate dependence on R from a crack closure effect unless the condition at which crack closure occurs is identified during testing.

Crack closure has been applied to explain the influence of R over various regimes of da/dN (Refs. 9–11, 13–15). However, most previous research was conducted on wrought test specimens that are not subject to the residual stresses prevalent in welded samples. An investigation of alloy steel arc welded joints for R ratios of 0.00 and 0.50 showed no increase in da/dN as R increased (Ref. 16). That is, the da/dN - ΔK curves essentially overlapped for all decades of crack growth. Since the test samples were oriented such that crack propagation occurred within the weld metal along the direction of welding, such behavior has been attributed to tensile residual stresses that were encountered within the weld metal. The presence of these tensile residual stresses promotes a completely open fatigue crack at all stages of loading. That is, crack closure, or premature closure of the crack tip during loading, would not be expected to influence the crack growth behavior.

To correctly evaluate the influence of crack closure, accurate assessment of the crack opening load, P_{op} , during testing is crucial as it serves as the foundation for

KEY WORDS

Residual Stress
Crack Initiation
Crack Growth
Stainless Steel
Gas Metal Arc
K-Increasing Test

C. S. KUSKO is Research Assistant; J. N. DUPONT is Associate Professor and Director, Joining and Laser Processing Laboratory; and A. R. MARDER is Professor, Department of Materials Science and Engineering, Lehigh University, Bethlehem, Pa.

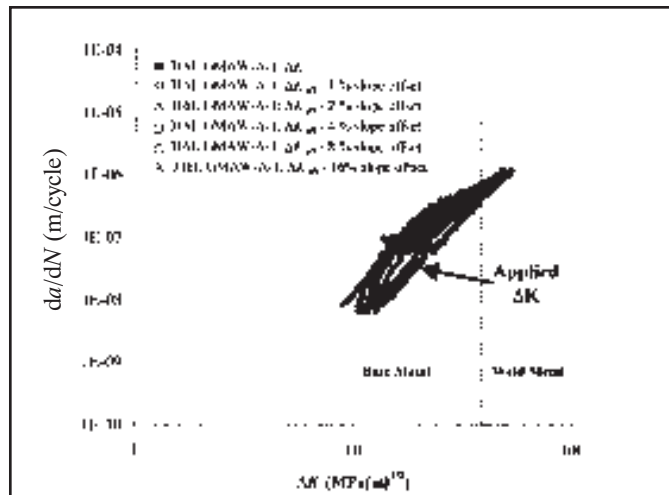
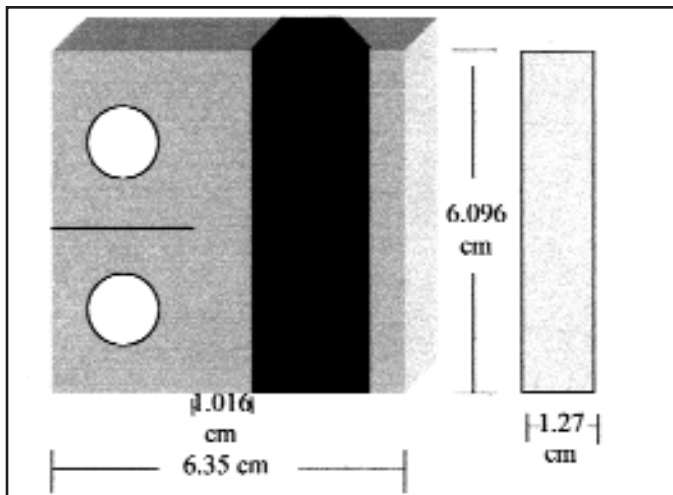


Fig. 1 — Schematic illustrations of C(T) specimens corresponding to gas metal arc weld of AB orientation. Fig. 2 — Slope offset data for 316L GMAW tested at an R ratio of 0.10.

Table 1 — Chemical Compositions (in wt-%) of 316L Base Metal and Filler Metal

	316L SS Base Metal	316L Filler Metal
Ni	10.16	12.17
Cr	16.12	18.20
Fe	68.85	64.43
Mo	2.05	2.53
Mn	1.71	1.66
Cu	0.44	0.10
Si	0.41	0.86
C	0.017	0.016
P	0.027	0.017
S	0.0011	0.014

Table 2 — Gas Metal Arc Welding Parameters

Parameter	Value
Base metal	316L
Backing bar	316L
Welding wire	316L
Welding wire diameter, mm	1.5875
Voltage, V	25–26
Current, A	280
Wire speed, cm/min	469.9
Carriage speed, cm/min	38.10
Welding position	flat
Shielding gas	98%Ar/2%O ₂
Number of layers	6
Number of passes	16
Preheat temp, °C	24
Interpass temp, °C	149

K_{op} and concomitant ΔK_{eff} calculations. A standardized compliance-based slope offset method has been previously utilized for the investigation of both ΔK and ΔK_{eff} for homogeneous wrought aluminum test specimens (Ref. 17). However, this method has yet to be systematically applied to welds that are susceptible to sig-

nificant residual stresses. The purpose of this research is to investigate the fatigue crack propagation behavior of stainless steel gas metal arc welds in order to observe how R influences such behavior.

Experimental Procedure

The 316L base metal and filler metal compositions used to prepare the weld samples are provided in Table 1. Weld samples were prepared by gas metal arc welding on base metals (dimensions 1.905 \times 15.24 \times 60.96 cm) by deposition of multiple passes on an automatic table using a 90-deg torch angle to the plate. The contact tip distance varied from 19.05 mm at the root to 12.70 mm from mid-plate to cap because of the addition of subsequent filler metal passes. Table 2 provides further details on the processing parameters.

Compact tension (C(T)) test specimens required for fatigue crack propagation testing were removed from the gas metal arc welds. Specimen dimensions conformed to those stated in American Society for Testing and Materials (ASTM) Standard E647 (Ref. 19). Figure 1 shows a schematic illustration of final dimensions, along with specimen orientation with respect to the fatigue crack starter notch and welding direction. The crack starter notch was inserted within the base metal normal to the direction of welding such that the distance from the end of the notch to the start of the weld metal on the front face was approximately 1.016 cm. The fatigue crack starter notch of length 2.54 cm, diameter 0.1524 mm, and radius of curvature 0.0762 mm was inserted by wire electrical-discharge machining (EDM). The configuration illustrated in Fig. 1 is designated as orientation AB. This two-letter system for

describing weld C(T) specimen orientation was utilized by James and co-workers (Refs. 21, 22) and is based on the designations adopted for wrought specimens by ASTM in Standard E399 (Ref. 23). In this system, the first letter represents the direction of applied loading while the second letter represents the direction of crack extension. In addition, A, B, and C symbolize the direction of welding, normal to the direction of welding, and the thickness direction, respectively. It has been observed that orientation AB, for which crack propagation occurs normal to the welding direction, would be most affected by residual stresses (Ref. 22).

All fatigue crack propagation testing was conducted in accordance with ASTM E647. Compliance measurements were recorded on both loading and unloading portions of the load-displacement curve. For the C(T) specimen, the following polynomial expression was utilized for determination of the normalized crack length, a/W , as a function of compliance, $BE\delta/P$ (Ref. 24).

$$\frac{a}{W} = 1.00098 - 4.66951X + 18.4601X^2 - 236.825X^3 + 1214.88X^4 - 2143.57X^5 \quad (2)$$

where (Ref. 24)

$$X = \frac{1}{\left[\frac{BE\delta}{P} \right]^{\frac{1}{2}} + 1} \quad (3)$$

In Equation 3, E is the modulus of elasticity. The term $BE\delta/P$ is referred to as the normalized compliance and is measured as a function of N . Once a/W has been cal-

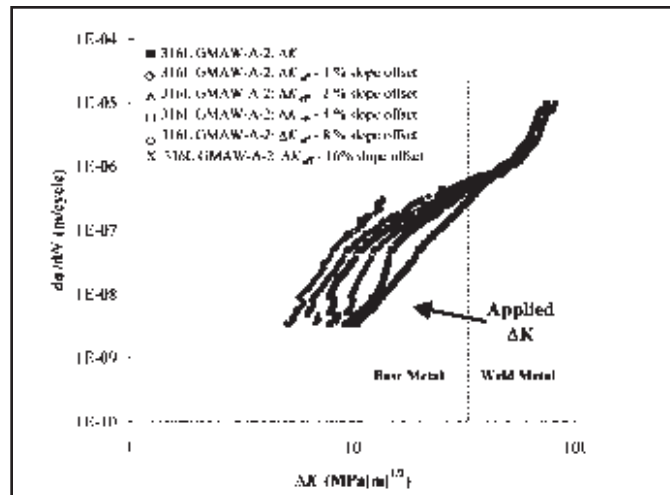
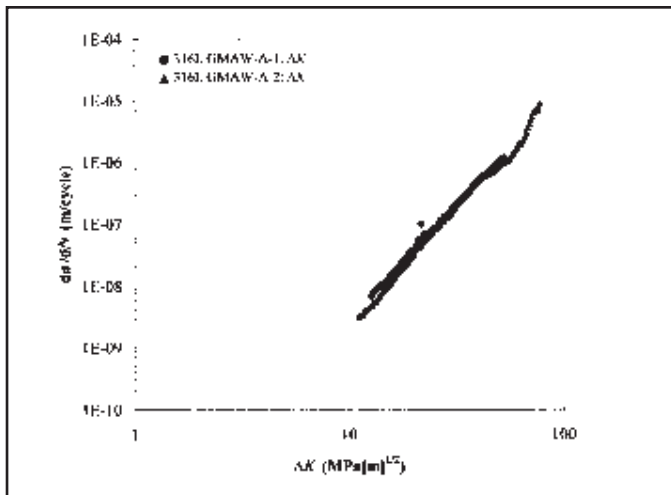


Fig. 3 — Comparison of 316L GMAW fatigue data tested at an R ratio of 0.10. Fig. 4 — Slope offset data for 316L GMAW tested at an R ratio of 0.10.

culated from Equation 2, the following expression developed for the C(T) specimen was used to calculate K (Ref. 25)

$$\frac{KBW^{\frac{1}{2}}}{P} = \frac{2 + \frac{a}{W}}{1 - \frac{a}{W}} \left[0.886 + 4.64 \frac{a}{W} - 13.32 \frac{a^2}{W^2} + 14.72 \frac{a^3}{W^3} - 5.6 \frac{a^4}{W^4} \right] \quad (4)$$

Displacement was measured using an MTS clip gauge attached to knife-edges on the front edge of the C(T) specimen.

All testing was conducted using constant amplitude loading and a sine waveform at a frequency of 25 Hz at room temperature. Testing was performed under K -gradient control at constant R ratios of various magnitudes to determine the influence on fatigue crack growth. Data were generated using K -increasing procedures (Ref. 26), according to the equation (Ref. 24)

$$K_{\max} = K_{\max,0} e^{C(a-a_0)} \quad (5)$$

where C , the normalized K -gradient, represents the fractional rate of change with increasing a , such that (Ref. 27)

$$C = \frac{1}{K_{\max}} \frac{dK_{\max}}{da} \quad (6)$$

The K -increasing tests were run with a C value of 0.118 mm^{-1} . On all samples, pre-cracking was conducted until the crack propagated 1.27 mm, after which, all ensuing da/dN were measured. The compliance-based crack lengths, measured as a function of N , were converted to da/dN using a modified version of the secant method (Ref. 28), which requires the calculation of the slope of a straight line connecting specified points on the a - N curve.

Results and Discussion

Fatigue Crack Propagation Results

Fatigue crack propagation data obtained from testing at an R ratio of 0.10 are shown in Fig. 2. The dotted line in the figure denotes the location where the fatigue crack crossed from the base metal into the weld metal. The solid black squares represent applied da/dN - ΔK data. The open symbols correspond to ΔK_{eff} data generated for various slope offset levels from 1% to 16% obtained from the compliance-based slope offset method, as described in Ref. 17. In this figure, the ΔK_{eff} curve for 1% slope offset level is farthest from the applied ΔK curve, while the ΔK_{eff} curve for 16% slope offset data is closest to the applied ΔK data. As explained in Ref. 17, the slope offset method may generate “artificial” crack closure information even if closure is not actually influencing crack growth. Such artificial measurements are easily identified through analysis of da/dN - ΔK and ΔK_{eff} curves for the various slope offset levels (Ref. 17) in the following manner. Once

all slope offset curves are plotted, it is determined whether unique slope offset curves result for each slope offset level or a single, overlapping curve is present for all slope offset levels. Unique da/dN curves for each slope offset level, as shown for most of the crack growth rates in Fig. 2, indicate legitimate crack closure data, signifying true crack closure. However, overlap of all slope offset level curves indicates that the software has “artificially” generated crack closure data, thus indicating that the crack is fully open and the effective stress intensity range is equal to the applied stress intensity range.

In Fig. 2, unique da/dN curves are evident for each slope offset level up to da/dN of $\sim 10^{-6}$ m/cycle. Thus, crack closure is significantly influencing crack growth behavior up to this level of crack growth rate at an R ratio of 0.10. At da/dN greater than $\sim 10^{-6}$ m/cycle, the slope offset curves for the five offset levels begin to converge to a single ΔK_{eff} curve, indicating that the crack is fully open beyond this growth rate. Under this condition, the K_{min} has increased to a point where it exceeds K_{op} and the crack is fully open in the growth rate regime above $\sim 10^{-6}$ m/cycle.

A second specimen of 316L weld was tested at an R ratio of 0.10 (over a wider crack growth rate) in order to assess the reproducibility of the results. The applied da/dN - ΔK curves for the two tests are shown in Fig. 3 and exhibit good agreement. In addition, Fig. 4 shows compliance offset data. These results are also in good agreement with Fig. 2, verifying a significant influence of crack closure during testing at $R = 0.10$ up to growth rates of $\sim 10^{-6}$ m/cycle, at which point the curves converge, and the crack is fully open above a growth rate of $\sim 10^{-6}$ m/cycle. Thus, only one specimen was tested at each of the remaining R ratios.

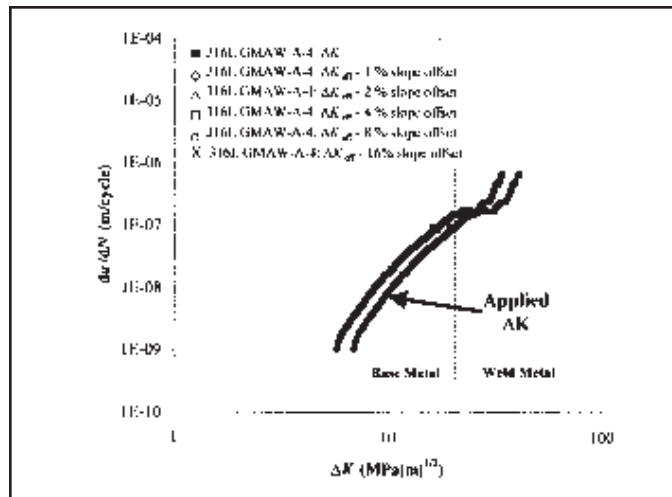
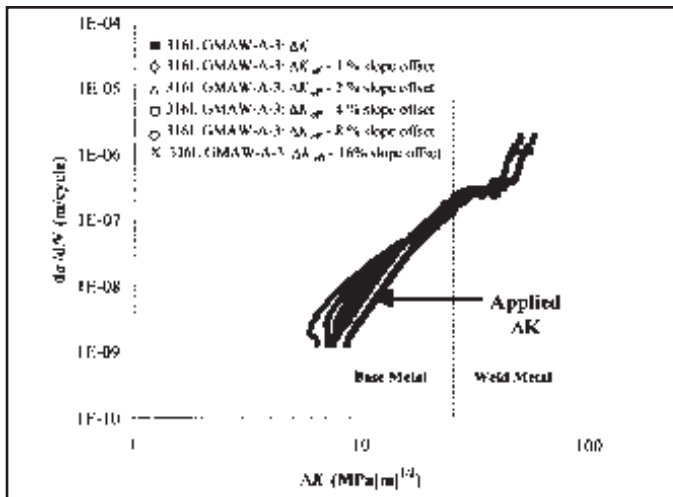


Fig. 5 — Slope offset data for 316L GMAW tested at an R ratio of 0.40.

Fig. 6 — Slope offset data for 316L GMAW tested at an R ratio of 0.55.

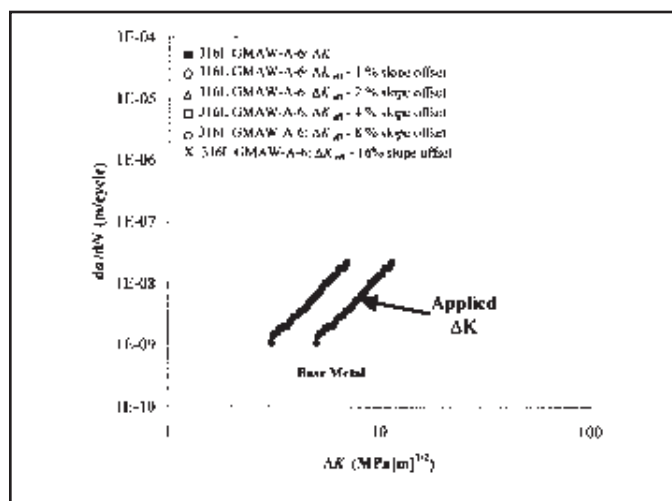
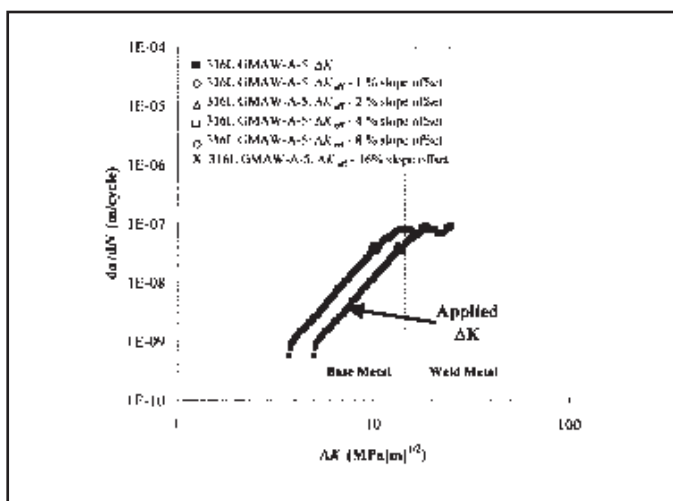


Fig. 7 — Slope offset data for 316L GMAW tested at an R ratio of 0.70.

Fig. 8 — Slope offset data for 316L GMAW tested at an R ratio of 0.80.

Based on the results of Figs. 2 and 4, the R ratio was increased to higher values in an attempt to overcome closure. These results are shown in Figs. 5–8. Figure 5 ($R = 0.40$) shows a true influence of crack closure below much lower da/dN values ($\sim 5 \times 10^{-8}$ m/cycle) than Figs. 2 and 4. Thus, because of the higher stress intensity ratio, K_{min} exceeds K_{op} at much lower crack growth rates and forces the crack to remain open at lower growth rates. Figure 6 ($R = 0.55$) exhibits a single ΔK_{eff} curve for all slope offset levels (i.e., only one offset curve is visible in the figure because all the offset curves lie on top of one another), indicating the crack is always fully open and $\Delta K = \Delta K_{eff}$ over the entire growth rate regime. As exhibited in Figs. 7 and 8, closure is also overcome for all da/dN at R ratios corresponding to 0.70 and 0.80. Figure 9 shows the applied da/dN - ΔK data from Figs. 2, 3, and 5–8 on a single plot. This figure illustrates that as

the R ratio increases, da/dN also increases for a given ΔK . For each respective R ratio test, this behavior occurs up to a specific da/dN at which the curves appear to coincide. The samples tested at R ratios of 0.70 and 0.80 exhibit crack growth rates that are similar over a wide range of crack growth rates.

Influence of R Ratio on Crack Growth Behavior

Figure 9 illustrates a general increase in da/dN with R for a given ΔK up to the point where $R = 0.70$. The curves corresponding to R ratios of 0.70 and 0.80 are essentially equivalent, while the curves for R ratios of 0.10, 0.40, and 0.55 show dependence on R . The dependence of da/dN on the R ratio at lower da/dN , followed by a convergence to a single curve at higher da/dN , has been previously observed for wrought aluminum alloys (Ref. 10). How-

ever, relatively little research has been conducted on stainless steel welded specimens. In addition, the condition at which the crack is partially closed is not always identified and, as a result, it is often not possible to separate an extrinsic effect of R (i.e., crack closure) from a true intrinsic, material behavior effect. In this work, identification of closure conditions permits separation of closure effects from true material dependence of crack growth rate on R . An influence of R has been observed for 304 austenitic stainless steel for a series of R ratios ranging from 0.05 to 0.75 at elevated temperatures (Ref. 4). That work was completed on wrought specimens rather than welds and did not consider crack closure measurements. Thus, based on the limited available research of austenitic stainless steel welds, it is useful to verify whether crack closure can explain the influence of R ratio on da/dN for these welded specimens.

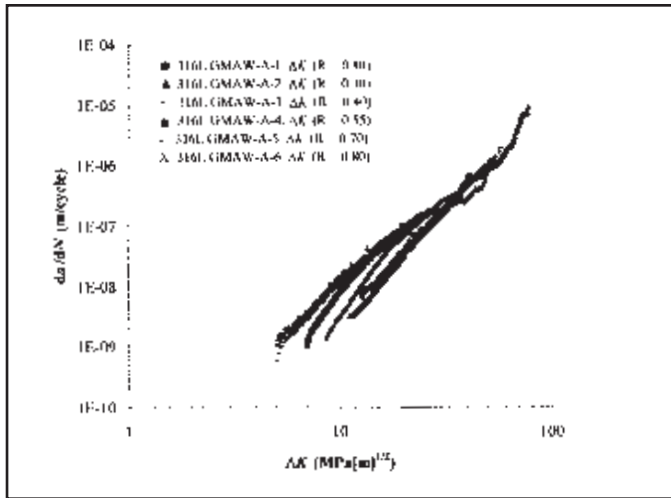


Fig. 9 — 316L GMAW data tested at a series of R ratios.

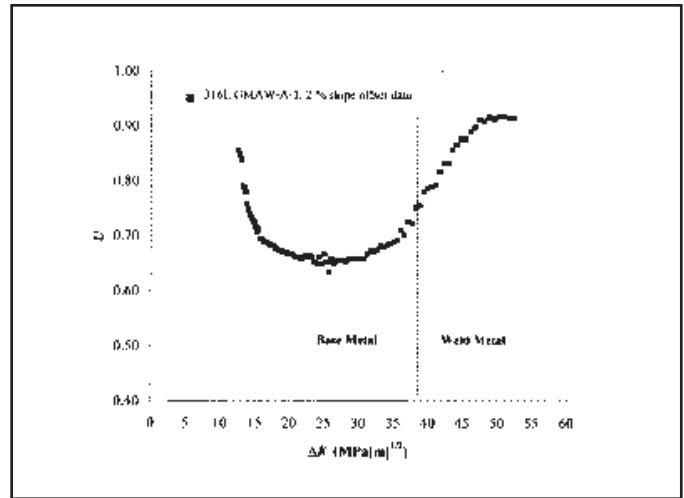


Fig. 10 — U vs. ΔK for 2% slope offset data for 316L GMAW tested at $R = 0.10$.

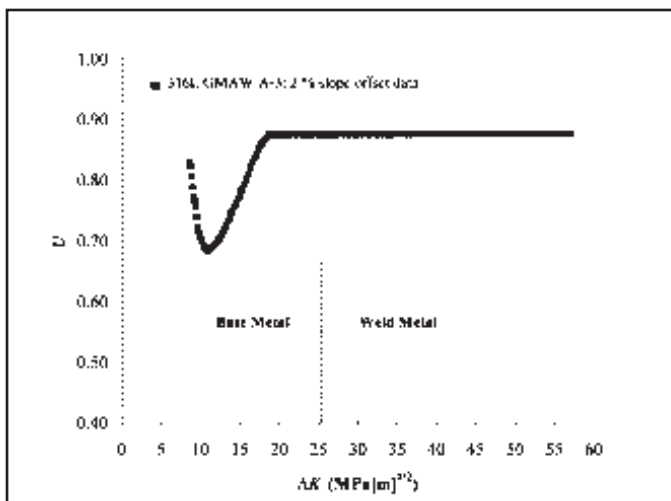


Fig. 11 — U vs. ΔK for 2% slope offset data for 316L GMAW tested at $R = 0.40$.

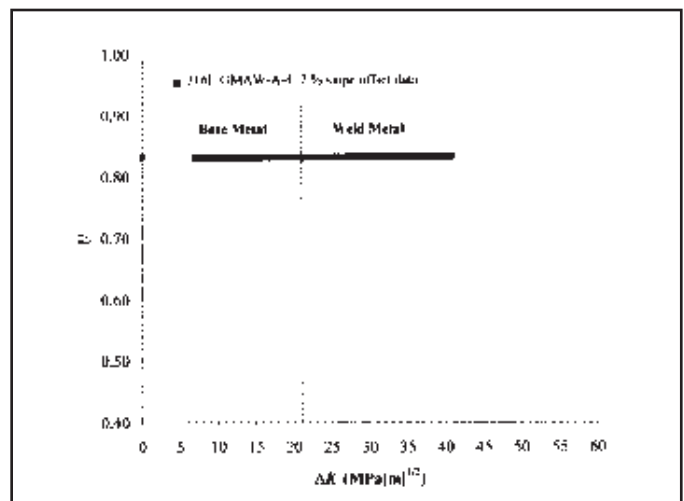


Fig. 12 — U vs. ΔK for 2% slope offset data for 316L GMAW tested at $R = 0.55$.

Crack closure behavior can be quantitatively characterized by the effective stress range ratio, U , which is defined as the ratio of ΔK_{eff} to ΔK (Ref. 31). As U increases toward a value of unity, the influence of crack closure diminishes. In other words, a value of U equal to one represents a completely open crack and a condition in which the applied stress intensity range, ΔK , is equal to the effective stress intensity range, ΔK_{eff} . As U decreases, the crack is closed during a larger portion of the loading cycle, and crack closure has a larger influence on the growth rate. Such knowledge can be applied to the da/dN data shown in Fig. 9 to determine if crack closure explains the da/dN dependence on R . Figure 10 illustrates the relationship between U and ΔK for the 316L weld tested at an R ratio of 0.10. In this figure, only 2% slope offset data are presented, as this offset level has been recommended as the most accurate (Ref. 17).

Since, as previously discussed, the

compliance offset software generates artificial crack closure measurements even when crack closure is not actually being detected, ΔK_{eff} will appear to have a value that differs in magnitude from ΔK even when the crack is fully open. However, these values are actually equal when there is no influence from crack closure. Consequently, for the current analysis, U will never actually equal a value of one. However, closure-free conditions are easily identified when U becomes constant and nearly equal to unity. For example, in Fig. 10, a closure-free condition is identified as the horizontal portion of the curve where U is constant and equal to 0.92, which occurs over limited ΔK above approximately 50 $\text{MPa}\sqrt{\text{m}}$. This figure verifies the dominant influence of crack closure for the weld samples tested at an R ratio of 0.10. Over a significant range of ΔK (approximately 14 $\text{MPa}\sqrt{\text{m}}$ to 26 $\text{MPa}\sqrt{\text{m}}$), U decreases with an increase in ΔK . That is, the

crack closure level initially increases with ΔK at lower ΔK . This can most likely be attributed to the crack entering a compressive residual stress field in the base metal from welding. However, as ΔK increases, K_{min} starts to approach K_{op} and the level of crack closure decreases (U increases). This trend continues until $U = 0.92$, at which point K_{min} exceeds K_{op} ; closure is overcome completely, and the crack is fully open. Thus, the increase in U and corresponding decreases in crack closure can be attributed to the increase in applied ΔK and/or the crack beginning to enter a residual tensile stress field.

As shown in Fig. 9, applied da/dN - ΔK increases for a given ΔK when R increases from 0.10 to 0.40. Figure 11 shows U as a function of ΔK for 2% slope offset data for an R ratio of 0.40. This plot exhibits the same behavioral trend as Fig. 10. U initially decreases with increasing ΔK prior to reaching a ΔK at which U escalates with

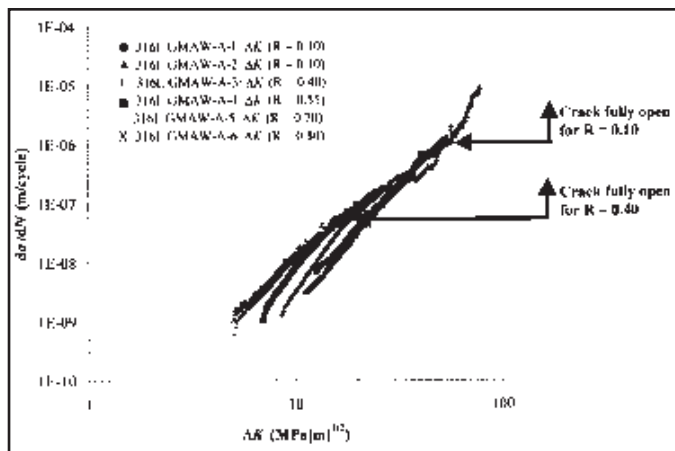


Fig. 13 — Replot of Fig. 9 showing locations where the crack becomes fully open for R ratios of 0.10 and 0.40.

ΔK . However, for an R ratio of 0.40, the ΔK at which this change occurs is approximately 10 MPa \sqrt{m} , which is considerably less than the ΔK of 25 MPa \sqrt{m} at which similar behavior transpires for an R ratio of 0.10. For comparison to the first two R ratios, Fig. 12 exhibits the U - ΔK relationship for the 2% offset level for an R ratio of 0.55. The single, horizontal line is indicative of artificial crack closure, and therefore, a completely open crack. Similar behavior was observed for R ratios of 0.70 and 0.80.

With this information in mind, a more detailed interpretation of Fig. 9 is now possible. Figure 13 shows a replot of Fig. 9. In this figure, the point at which crack closure is overcome for R ratios of 0.10 and 0.40 are noted on the figure. For an R ratio of 0.10, the crack is fully open at fatigue crack growth rates above 1×10^{-6} m/cycle. For an R ratio of 0.40, the crack is fully open at fatigue crack growth rates above 5×10^{-8} m/cycle. For the remaining R ratios, the crack is always open. First, note that the crack growth rates are essentially independent of R at growth rates above $\sim 1 \times 10^{-6}$ m/cycle, which is commonly observed since R has the largest influence on da/dN at low ΔK values. Below this growth rate, the crack is not fully open for an R value of 0.10. Thus, the increase in growth rate which occurs as R is increased from 0.10 to 0.40 can be attributed to an extrinsic effect. In other words, this increase in da/dN is caused by overcoming crack closure and is not an intrinsic material effect. A similar argument can be made for an R ratio of 0.40 at growth rates below 5×10^{-8} m/cycle, where the increase in da/dN which is observed as R is increased from 0.40 to 0.55 is due to overcoming crack closure. However, even though the crack is always open for the remaining R values of 0.55, 0.70, and 0.80, an increase in growth rate is observed as R in-

creases from 0.55 to 0.70 up to a growth rate of approximately 3×10^{-8} m/cycle. Thus, the increase in growth rate which is observed as R increases from 0.55 to 0.70 within this growth rate regime is a true intrinsic material response to the increase in stress ratio. No significant further material response in da/dN is observed as R is increased further from 0.70 to 0.80.

Summary and Conclusions

The influence of R ratio on the fatigue crack propagation behavior of stainless steel gas metal arc welds was evaluated. The compliance offset method was applied to gas metal arc weld specimens in order to explain the influence of R ratio on crack growth behavior. For the stainless steel gas metal arc welds evaluated, an R ratio of 0.55 has been shown to overcome crack closure over all growth rate regimes. Increases in crack growth rates as R is increased from 0.10 to 0.55 can generally be attributed to an extrinsic effect in which crack closure is overcome. In contrast, the increase in crack growth rate observed for an increase in R from 0.55 to 0.70 is a true intrinsic material response. Further increase in R from 0.70 to 0.80 produces no significant enhancement in the fatigue crack growth rates.

Acknowledgments

The authors thank the United States Office of Naval Research for providing funding for this research. The authors would also like to acknowledge Mike Rex, John Gregoris, and Gene Kozma at Lehigh University for assistance with fatigue crack propagation sample preparation and testing. Preparation of the gas metal arc weld samples by Ravi Menon at Stoddy Co. in Bowling Green, Ky., is also greatly appreciated.

References

1. Maddox, S. J. 1970. *Metal Construction and British Welding Journal*, Vol. 2, pp. 285–289.
2. Parry, M., Nordberg, H., and Hertzberg, R. W. 1972. *Welding Journal* 51(10): 485-s to 490-s.
3. Paris, P. C. 1964. Fatigue — An Interdisciplinary Approach. *Proc. of the 10th Sagamore Army Materials Research Conference*, Eds. J. J. Burke, N. L. Reed, and V. Weiss, pp. 107–132.

4. James, L. A. 1972. *Nuclear Technology* 14: 163–170.
5. Cooke, R. J., and Beevers, C. J. 1973. *Engineering Fracture Mechanics* 5: 1061–1071.
6. Ohta, A., and Sasaki, E. 1977. *Engineering Fracture Mechanics* 9: 655–662.
7. Ohta, A., and Sasaki, E. 1977. *Engineering Fracture Mechanics* 9: 307–315.
8. Ohta, A., Sasaki, E., Kamakura, M., Nihei, M., Kosuge, M., Kanao, M., and Inagaki, M. 1981. *Transactions of the Japan Welding Society* 12: 31–38.
9. Katcher, M., and Kaplan, M. 1974. Fracture toughness and slow-stable cracking. ASTM STP 559, American Society for Testing and Materials, pp. 264–292.
10. Brown, R. D., and Weertman, J. 1978. *Engineering Fracture Mechanics* 10: 757–771.
11. Vazquez, J. A., Morrone, A., and Ernst, H. 1979. *Engineering Fracture Mechanics* 12: 231–240.
12. Stofanek, R. J., Hertzberg, R. W., Miller, G., Jaccard, R., and Donald, K. 1983. *Engineering Fracture Mechanics* 17: 527–539.
13. Lindley, T. C., and Richards, C. E. 1974. *Materials Science and Engineering* 14: 281–293.
14. Boute, N. F., and Dover, W. D. 1977. *Fracture* 1977 2: 1065–1071.
15. Clerivet, A., and Bathias, C. 1979. *Engineering Fracture Mechanics* 12: 599–611.
16. Ohta, A., Suzuki, N., and Maeda, Y. 1977. *International Journal of Fatigue* 19: S303–S310.
17. Donald, J. K. 1988. Mechanics of fatigue crack closure. ASTM STP 982. Eds. C. Newman, Jr., and W. Elber. American Society for Testing and Materials, pp. 222–229.
18. Banovic, S. W., DuPont, J. N., and Marder, A. R. 2001. *Metallurgical Transactions B* 32B: 1171–1176.
19. *Annual Book of ASTM Standards*. Vol. 3.01. 1996. ASTM E647 Section 3. Metals test and analytical procedures. American Society for Testing and Materials: Materials Park, Ohio, pp. 565–601.
20. Hickman, G. 2000. Allegheny Ludlum, Private communication.
21. James, L. A. 1973. *Welding Journal*, 52(3): 173-s to 179-s.
22. James, L. A., and Mills, W. J. 1987. *Welding Journal* 66(8): 229-s to 234-s.
23. *Annual Book of ASTM Standards*. Vol. 03.01. 1996. ASTM E399, Section 3: Metals test methods and analytical procedures. ASM International: Materials Park, Ohio, pp. 407–437.
24. Saxena, A., and Hudak, S. J., Jr. 1978. *International Journal of Fracture* 14: 453–468.
25. Srawley, J. E. 1976. *International Journal of Fracture* 12: 475–476.
26. Donald, J. K., and Schmidt, D. W. 1980. *Journal of Testing and Evaluation* 8: 19–24.
27. Saxena, A., Hudak, S. J., Jr., Donald, J. K., and Schmidt, D. W. 1978. *Journal of Testing and Evaluation* 6: 167–174.
28. Clark, W. G., Jr., and Hudak, S. J., Jr. 1975. *Journal of Testing and Evaluation* 3: 454–476.
29. Shih, Y. W., Chen, B. Y., and Zhang, J. X. 1990. *Engineering Fracture Mechanics* 36: 893–902.
30. Donald, K. 2002. Fracture Technology Associates, Private communication.
31. Elber, W. 1971. Damage tolerance in aircraft structures. ASTM STP 486, American Society for Testing and Materials, pp. 230–242.
32. Frost, N. E., Pook, L. P., and Denton, K. 1971. *Engineering Fracture Mechanics* 3: 109–126.